



# An elastic framework for ensemble-based large-scale data assimilation

Sebastian Friedemann, Bruno Raffin

## ► To cite this version:

Sebastian Friedemann, Bruno Raffin. An elastic framework for ensemble-based large-scale data assimilation. [Research Report] RR-9377, INRIA : Institut national de recherche en sciences et technologies du numérique. 2020, pp.1-28. hal-03017033v2

**HAL Id: hal-03017033**

**<https://hal.inria.fr/hal-03017033v2>**

Submitted on 24 Nov 2020 (v2), last revised 14 Jun 2022 (v3)

**HAL** is a multi-disciplinary open access archive for the deposit and dissemination of scientific research documents, whether they are published or not. The documents may come from teaching and research institutions in France or abroad, or from public or private research centers.

L'archive ouverte pluridisciplinaire **HAL**, est destinée au dépôt et à la diffusion de documents scientifiques de niveau recherche, publiés ou non, émanant des établissements d'enseignement et de recherche français ou étrangers, des laboratoires publics ou privés.



# An elastic framework for ensemble-based large-scale data assimilation

Sebastian Friedemann, Bruno Raffin

**RESEARCH  
REPORT**

**N° 9377**

November 2020

Project-Team DataMove

ISRN INRIA/RR--9377--FR+ENG

ISSN 0249-6399





# An elastic framework for ensemble-based large-scale data assimilation

Sebastian Friedemann, Bruno Raffin

Project-Team DataMove

Research Report n° 9377 — November 2020 — 28 pages

## Abstract:

Prediction of chaotic systems relies on a floating fusion of sensor data (observations) with a numerical model to decide on a good system trajectory and to compensate nonlinear feedback effects. Ensemble-based data assimilation (DA) is a major method for this concern depending on propagating an ensemble of perturbed model realizations.

In this paper we develop an elastic, online, fault-tolerant and modular framework called Melissa-DA for large-scale ensemble-based DA. Melissa-DA allows elastic addition or removal of compute resources for state propagation at runtime. Dynamic load balancing based on list scheduling ensures efficient execution. Online processing of the data produced by ensemble members enables to avoid the I/O bottleneck of file-based approaches. Our implementation embeds the PDAF parallel DA engine, enabling the use of various DA methods. Melissa-DA can support extra ensemble-based DA methods by implementing the transformation of member background states into analysis states. Experiments confirm the excellent scalability of Melissa-DA, running on up to 16,240 cores, to propagate 16,384 members for a regional hydrological critical zone assimilation relying on the ParFlow model on a domain with about 4 M grid cells.

**Key-words:** Data Assimilation, Ensemble Kalman Filter, Ensemble, Multi Run Simulations, Elastic, Fault Tolerant, Online, In Transit Processing, Master/Worker

RESEARCH CENTRE  
GRENOBLE – RHÔNE-ALPES

Inovallée  
655 avenue de l'Europe Montbonnot  
38334 Saint Ismier Cedex

# An elastic framework for ensemble-based large-scale data assimilation

## 1 Introduction

Numerical models of highly nonlinear (chaotic) systems (e.g., the atmospheric, the oceanic or the ground water flow) are extremely sensitive to input variations. The goal of data assimilation (DA) is to reduce the result uncertainty by correcting the model trajectory using observation data.

Two main approaches are used for DA, variational and statistical [2, 25]. In this paper we focus on statistical ensemble-based DA, where an ensemble of several model instances is executed to estimate the model error against the observation error. Various methods exist for that purpose like the classical Ensemble Kalman Filter (EnKF) we use for experiments in this paper.

Combining large numerical models and ensemble-based DA requires execution on supercomputers. Recent models have millions of degrees of freedom, but only hundreds of ensemble members are used for operational DA. Thus today's approaches suffer from undersampling: to minimize and to estimate the sampling error, much larger ensembles with thousands of members would be necessary. Current approaches rely either on files to aggregate the ensemble results and send back corrected states or on the MPI message passing programming paradigm to harness the members and the assimilation process in a large monolithic code, but these approaches are not well-suited to running ultra-large ensembles on the coming exascale computers. Efficient execution at exascale requires mechanisms to allow dynamic adaptation to the context, including load balancing for limiting idle time, elasticity to adapt to the machine availability, fault tolerance to recover from failures caused by numerical, software or hardware issues and direct communications between components instead of files to bypass the I/O performance bottleneck.

This paper proposes a novel architecture characterized by its flexibility and modularity called Melissa-DA. Experiments using the ParFlow parallel hydrology solver on a domain with about 4 M grid cells as numerical model were run with up to 16,384 members on 16,240 cores. Each member itself was parallelized on up to 48 MPI ranks. Melissa-DA adopts a three-tier architecture based on a launcher in charge of orchestrating the full application execution, independent parallel runners in charge of executing members up to the next assimilation update phase, and a parallel server that gathers and updates member states to assimilate observation data into them. The benefits of this framework include:

- **Elasticity:** Melissa-DA enables the dynamic adaptation of compute resource usage according to availability. Runners are independent and connect dynamically to the parallel server when they start. They are submitted as independent jobs to the batch scheduler. Thus, the number of concurrently running runners can vary during the course of a study to adapt to the availability of compute resources.

- **Fault tolerance:** Melissa-DA’s asynchronous master/worker architecture supports a simple yet robust fault tolerance mechanism. Only some lightweight book-keeping and a few heartbeats as well as checkpointing on the server side are required to detect issues and restart the server or the runners.
- **Load balancing:** The distribution of member states to runners is controlled by the server and defined dynamically according to a list scheduling algorithm, enabling to adjust the load of each runner according to the time required to propagate each member.
- **Online processing:** Exchange of state variables between the different parts of the Melissa-DA application and the different parts of an assimilation cycle happens fully online avoiding file system access and its latency.
- **Communication/computation overlap:** Communications between the server and the runners occur asynchronously, in parallel with computation, enabling an effective overlapping of computation and communication, improving the overall execution efficiency.
- **Code modularity:** Melissa-DA enforces code modularity by design, leading to a clear separation of concern between models and DA. The runners execute the members, i.e., model instances, while the server, a separate code running in a different job, is concerned with observation processing and running the core DA algorithm.

After a quick reminder about statistical data assimilation and especially the Ensemble Kalman Filter (section 2), related work is presented (section 3). The proposed architecture and the Melissa-DA framework are detailed (section 4) before analyzing experimental results (section 5). A conclusion closes the paper (section 6).

## 2 Statistical data assimilation and the ensemble Kalman filter

We survey the base concepts of ensemble-based data assimilation and the EnKF filter. Refer to [2] and [13] for more details.

The goal of DA is to estimate the real state of the system as accurately as possible merging model intermediate results and observations. This is critical in particular to models showing chaotic or semichaotic behavior, where small changes in the model input lead to large changes in the model output. The state estimate is called *analysis state*  $x_a$ . It might be an estimate of, e.g., the present atmospheric state in Numerical Weather Prediction (NWP) or the soil moisture field when calibrating hydrological ground water models using DA. The analysis state  $x_a$  is retrieved running a model (e.g., the atmospheric or hydrological model itself) and improving the model output using the observation vector  $y$ .

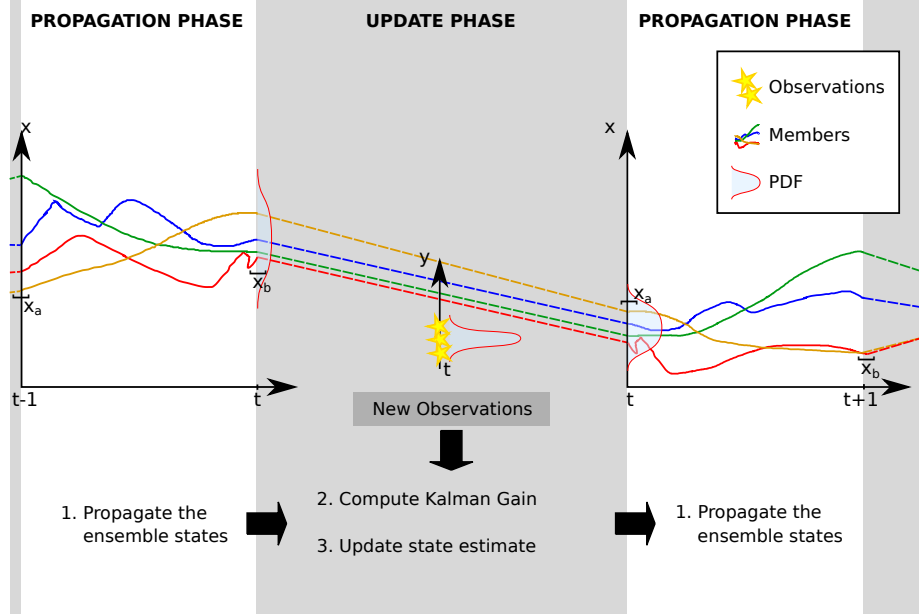


Figure 1: The ensemble Kalman filter workflow.

Observation vectors in the geoscientific domain typically contain a mix of values from remote sensing instruments (satellites) and in situ observations by ground based observatories, buoys, aircrafts etc.

Models operate on the system state  $x \in X \subseteq \mathbb{R}^N$  that cannot be directly observed. In the standard DA formalism, the model operator  $\mathcal{M}$  fulfills the Markov property, taking the present state  $x_t$  as its *only* input to produce the next state  $x_{t+1}$ :

$$x_{t+1} = \mathcal{M}(x_t). \quad (1)$$

To compare and weight an observation vector  $y \in Y \subseteq \mathbb{R}^K$ , and system state  $x$ , we rely on an observation operator  $\mathcal{H}$  that maps from model space to the observation space:

$$\tilde{y} = \mathcal{H}(x). \quad (2)$$

In the case where both, the model output probability density function (PDF) and the observation's PDF are known, multiplying the two and normalizing in Bayesian manner provides the analysis state PDF. Ensemble-based statistical DA estimates the model PDF by sampling an ensemble of model states and propagating these states through  $\mathcal{M}$ .

The *Ensemble Kalman Filter* (EnKF) is the most studied statistical ensemble-based DA method. This is the filter we rely on to validate the Melissa-DA approach, and its workflow is common to many other DA filters. The EnKF inherits the Kalman Filter [19], extending it to non-linear models [2]. The different steps of EnKF assimilation cycles are the following (Figure 1):

1. An ensemble  $X_a$  of  $M$  states ( $x_a^i | i \in [M]$ ), statistically representing the assimilated state, is propagated by the model  $\mathcal{M}$ . The obtained states are

the background states  $(x_b^i | i \in [M])$ . For the initial assimilation cycle  $X_a$  is an ensemble of perturbed states. Later it is obtained from the previous assimilation cycle.

2. The Kalman gain  $K$  is calculated from the ensemble covariance and the observation error  $R$ .
3. Multiply the Kalman gain  $K$  with the innovation  $(y - \mathcal{H}(x_b^i))$  and add to the background states:  $x_a^i = x_b^i + K \cdot (y - \mathcal{H}(x_b^i))$  to obtain the new ensemble analysis states  $(x_a^i | i \in [M])$ .
4. Start over with the next assimilation cycle (step 1).

### 3 Related work

DA techniques fall into two main categories, variational and statistical. Variational DA (e.g., 3D-Var and 4D-Var) relies on the minimization of a cost function evaluating the difference between the model state and the observations. Minimizing the cost function is done via gradient descent that requires adjoints for both the model and the observation operator. This approach is compute efficient, but the adjoints are not always available or may require significant efforts not always accessible. Nowadays large-scale DA applications as, e.g., used by Numerical Weather Prediction (NWP) operators typically rely on a variational DA. For instance, the China Meteorological Administration uses 4D-Var to assimilate about 2.1 million daily observations into a global weather model with more than 7.7 million grid cells. As in 2019, the DA itself is parallelized on up to 1,024 processes [40].

Statistical DA takes a different approach relying on an ensemble run of the model to compute an estimator of some statistical operators (co-variance matrix for EnKF, PDF for particle filters). This approach consumes more compute power as the number of members needs to be large enough for the estimator to be relevant, but stands for its simplicity as it only requires the model operator without adjoint as for the variational approach. But scaling the ensemble size can be challenging especially when the model is already time consuming and requires its own internal parallelization.

Two main approaches are used to handle. Either members run independently producing files that are read for the update phase, that itself produces new files read by members for the next assimilation cycle. This approach makes for a flexible workflow amenable to fault tolerance and adjustable resource allocations. Using files for data exchange simplifies the issue of data redistribution especially in the case where the parallelization level of a given member differs from the one implemented for the update (usually called a  $N \times M$  data redistribution). This approach is adopted by the EnTK framework [6], used to manage up to 4,096 members for DA on a molecular dynamics application [5] and by Toye et al. [38] assimilating oceanic conditions in the Red sea with  $O(1,000)$



members. The OpenDA framework also supports this *blackbox* model, relying on NetCDF files for data exchange for NEMO in [39]. However relying on the machine I/O capabilities using files is a growing performance bottleneck. In 10 years the compute power made a leap by a  $134\times$  factor, from 1.5 PFlop/s peak on Roadrunner (TOP500 #1 in 2008) to 201 PFlop/s peak on Summit (#1 in 2018), the I/O throughput for the same machines only increased by a  $12\times$  factor, from 204 GB/s to 2,500 GB/s. This trend is expected to continue at exascale. For instance the announced Frontier machine (2021) expected to reach 1 ExaFlop/s should offer 5 to 10 times the compute power of Summit but only 2 to 4 times its I/O throughput<sup>1</sup>.

The other approach builds a large MPI application that embeds and coordinates the propagation of the different members as well as the update phase. Data exchange relies on efficient MPI collective communications. The drawback is the monolithic aspect of this very large application. The full amount of resources needed must be allocated upfront and for the full duration of the execution. Making such application fault-tolerant and load balanced is challenging. Ensemble runs are particularly sensible to numerical errors as the ensemble size increases the probability that the model may execute in numerical domains it has not been well tested with. The frameworks DART [1] and PDAF [31] are based on this approach. PDAF for instance has been used for the ground water flow model TerrSysMP using EnKF with up to 256 members [23]. Other DA work rely on custom MPI codes. Miyoshi et al. [28] ran 10,240 members with the LENKF filter on the K-computer in 2014. In 2018, Berndt et al. assimilated up to 4,096 members with 262,144 processors and a particle filter, and production use case with 1,024 members for wind power prediction over Europe [8]. Variational and statistical DA can also be combined. NWP actors like the ECMWF, the British Met office and the Canadian Meteorological Centre rely on such approaches using hundreds of ensemble members to improve predictions [22, 11, 16].

Looking beyond DA frameworks, various Python based frameworks are supporting the automatic distribution of tasks, enabling to manage ensemble runs. Dask [34] is for instance used for hyperparameter search with Scikit-Learn, Ray [29] for reinforcement learning [24]. But they do not support tasks that are built from legacy MPI parallel codes. Other frameworks such as Radical-Pilot (the base framework of EnTK) [32] or Parsl [4] enable such features but are using files for data exchange. Other domain specific frameworks like Dakota [12], Melissa [37] or Copernicus [33] enable more direct support of parallel simulation codes but for patterns that require less synchronizations than the ones required for DA.

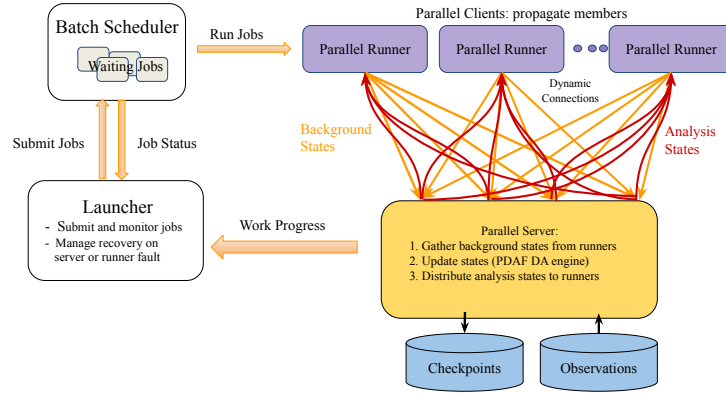


Figure 2: Melissa-DA three-tier architecture. The launcher supervises the execution in tight link with the batch scheduler. The job scheduler regulates the number of simulation jobs (runners) to run according to the machine availability, leading to an elastic resource usage. The server distributes the members to propagate to the connected runners dynamically for balancing their workload. A fault tolerance mechanism automatically restarts failing runners or a failing server.

## 4 Melissa-DA architecture

### 4.1 Overview

Melissa-DA relies on an elastic and fault-tolerant parallel client/server communication scheme, inheriting a three-tier architecture from Melissa [37], (Figure 2). The *server* gathers background states from all ensemble members. New observations are assimilated into these background states to produce a new analysis state for each member. These analysis states are distributed by the server to the *runners* that take care of progressing the ensemble members up to the next assimilation cycle. Member to runner distribution is adapted dynamically by the server according to the runner work loads, following a list scheduling algorithm. The runners and the server are parallel codes that can run with different numbers of processes. They exchange member states through  $N \times M$  communication patterns for efficiency purpose. These patterns map different runner domain parts stored by different runner ranks to server ranks. The server and the runners are launched independently in separate jobs by the machine batch scheduler. Runners connect dynamically to the server when starting. This master/worker architecture enables an elastic resource usage, as the number of runners can dynamically evolve depending on the availability of compute resources. The third tier is called *launcher*. The launcher orchestrates the execution, interacting with the supercomputer batch scheduler to request resources

<sup>1</sup>see <https://www.olcf.ornl.gov/frontier/>, retrieved the 03.11.2020

to start new jobs, kill jobs, monitor job statuses, and trigger job restarts in case of failure.

## 4.2 Member states

Often the observation operator  $\mathcal{H}$  in a DA framework only applies to one part of the whole model state vector. Thus the assimilated state vector denoted  $x$  only needs to contain this part of the full model state. Other model variables that affect state propagation are left unchanged by the update phase. To account for this distinction we split a model state vector into two main parts, the *static state* and the *dynamic state*, and we distinguish a sub-part of the dynamic state called the *assimilated state*. The static state encompasses all model variables defined at start-time that are left unchanged by model propagation. The static state is the same for all ensemble members. This may be the mesh topology used for spatial discretization, given it is invariant to model propagation and all members use the same. The union of the static and dynamic state is the full set of information needed by the model to propagate an ensemble member further in time. The assimilated state is the sub-part of the dynamic state that is required by the update phase of the assimilation process according to the available observations. We make this distinction as this is the base for the dynamic load balancing and fault tolerance mechanisms of Melissa-DA detailed in the following sections. Indeed, a Melissa-DA runner only keeps the static state for its whole lifetime, while the dynamic states of the members are exchanged between the server and the runners. The server can thus checkpoint a member saving its dynamic state only or assign a given member to a different runner by providing its dynamic state. Practically, properly identifying the dynamic state can be challenging for some applications.

## 4.3 Server

At every assimilation cycle the server collects the dynamic states of all ensemble members from the runners to calculate the next ensemble of analysis states. At the same time it works as a master for the runners, distributing the next ensemble member (dynamic) states to be propagated to the runners. The server is parallel (based on MPI) and runs on several nodes. The number of nodes required for the server is primarily defined by its memory needs. The amount of memory needed is in the order of the sum of the member dynamic states. As detailed in [subsection 4.2](#), the dynamic state (the state to be assimilated plus the extra simulation variables that differentiate a member from the other) is the minimal amount of information needed to restore a given member on any runner.

The server needs to be linked against a user defined function to initialize all the member states ([Figure 3](#) `init_ensemble`). Other functions, e.g., to load the current assimilation cycle observation data (`init_observations`) and the observation operator  $\mathcal{H}$  (`observation_operator_H`) must be provided to the server for each DA study. In the current version user functions are called sequentially

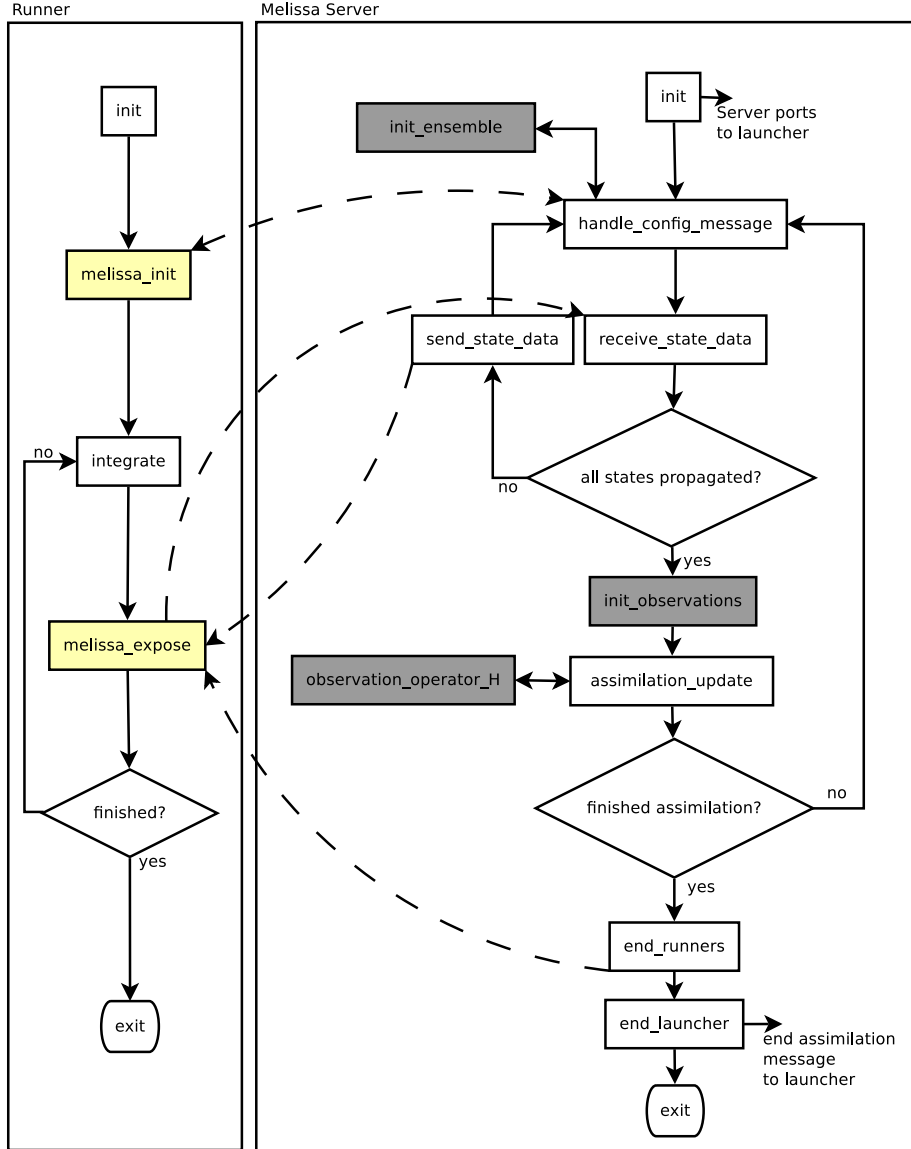


Figure 3: Melissa-DA runner and server interactions (fault tolerance part omitted for sake of clarity). Dashed arrows denote messages that are exchanged between different components. Grey boxes are methods that need to be implemented by the user. Yellow boxes are Melissa-DA API calls that need to be introduced in the simulation code to transform it into a runner.

by the server, but we expect to support concurrent calls to `init_ensemble` and `init_observations` to further improve the server performance.

The current server embeds PDAF as parallel assimilation engine. The server parallelization can be chosen independently from the runner parallelization. A

$N \times M$  data redistribution takes place between each runner and the server to account for different levels of parallelism on the server and runner side. This redistribution scheme is implemented on top of ZeroMQ, a connection library extending sockets [15]. This library supports a server/client connection scheme allowing dynamic addition or removal of runners.

Care must be taken to store the coherent state vector parts and simulation variables together as they might not be received by all server ranks in the same order, as runners are not synchronized. For instance server rank 0 could receive a part of ensemble state vector 3 while rank 1 receives a part of ensemble state vector 4. Even more importantly the state parts that are sent back must be synchronized so that the ranks of one runner receive the parts of the same ensemble state vector from all the connected server ranks. For that purpose all received state parts are labeled with the ensemble member ID they belong to, enabling the server to assemble coherently distributed member states. State propagation is ensured by the server rank 0, the only one making decisions on which runner shall propagate which ensemble member. This decision is next shared amongst all the server ranks using non blocking MPI broadcasts. This way communication between different server and runner ranks overlaps while other runner(ranks) perform unhindered model integration.

#### 4.4 Runners

Melissa-DA runners are based on the simulation code, instrumented using the minimalist Melissa-DA API. This API consists only of two functions: `melissa_init` and `melissa_expose` (Figure 3). `melissa_init` must be called once at the beginning to define the size of the dynamic state vector per simulation rank. This information is then exchanged with the server, retrieving the server parallelization level. Next `melissa_init` opens all necessary connections to the different server ranks.

`melissa_expose` needs to be inserted into the simulation code to enable extraction of the runner dynamic state and to communicate it with the server. When called, this function is given a pointer to the runner’s dynamic state data in memory that is sent to the server who saves it as background state. Next `melissa_expose` waits to receive from the server the dynamic part of an analysis state, used to update the runner dynamic state. The function `melissa_expose` returns the number of timesteps the received analysis state shall be propagated or a stop signal.

#### 4.5 Launcher

To start a Melissa-DA application, a user starts the launcher that then takes care of setting up the server and runners on the supercomputer.

The launcher typically runs on the supercomputer front node and is the only part of the Melissa-DA application that interacts with the machine batch scheduler. The launcher requests resources for starting the server job and as soon as the server is up it submits jobs for runners. Hereby it prioritizes job

submission within the same job allocation (if the launcher itself was started within such an allocation). Otherwise the launcher can also submit jobs as self contained allocations (by, e.g., calling `srun` outside of any allocation on Slurm based supercomputers). In the latter case it can happen that the server job and some runner jobs are not executed at the same time leading to inefficient small Melissa-DA runs. Thus ideally at least jobs for the server and some runners are launched within the same allocation ensuring the Melissa-DA application to operate efficiently even if no further runner jobs can be submitted. It is further also possible to instruct the launcher to start jobs within different partitions.

If the launcher detects that too few runners are up, it requests new ones, or, once notified by the server that the assimilation finished, it deletes all pending jobs and finishes the full application. The launcher also periodically checks that the server is up, restarting it from the last checkpoint if necessary. The notification system between the server and the launcher is based on ZeroMQ. There are no direct connections between runners and the launcher. The launcher only observes the batch scheduler information on runner jobs.

## 4.6 Fault tolerance

Melissa-DA supports detection and recovery from failures (including straggler issues) of the runners through timeouts, heartbeats and server checkpoints. Since the server stores the dynamic states of the different members and each runner builds the static state at start time, no checkpointing is required on the runners. So Melissa-DA ensures fault recovery even if the model simulation code does not support checkpointing. If supported, runners can leverage simulation checkpointing to speed-up runner restart.

The server is checkpointed using the FTI library [7], enabling the recovery from server crashes without user interaction. The server sends heartbeats to the launcher. If missing, the launcher kills the runner and server jobs and restarts automatically from the last server checkpoint. The server is also in charge of tracking runner activity based on timeouts. If a runner is detected as failing, the server re-assigns the current runner's member propagation to an other active runner. More precisely, if one of the server ranks detects a timeout from a runner, it notifies the server rank 0 that reschedules this ensemble member to a different runner, informing all server ranks to discard information already received by the failing runner. Further, the server sends stop messages to all other ranks of the failing runner. The launcher, also notified of the failing runner, properly kills it and requests the batch scheduler to start a new runner that will connect to the server as soon as ready.

One difficulty are errors that cannot be solved by a restart, typically numerical errors or, e.g., a wrongly configured server job. To circumvent these cases Melissa-DA counts the number of restarts. If the maximum, a user defined value, is reached, Melissa-DA stops with an informative error message. In the case of a recurrent error on a given member state propagation, it is possible to avoid stopping the full application. One option is to automatically replace such members with new ones by calling a user defined function for generating new

member states, possibly by perturbing existing ones. Alternatively when the maximum number of restarts for a member state propagation is reached, this member could simply be canceled. As the number of members is high, removing a small number of members usually does not impair the quality of the DA process. These solutions remain to be implemented in Melissa-DA.

A common fault are jobs being canceled by the batch scheduler once reaching the limit walltime. If this occurs at the server or runner level, the fault tolerance protocol operates.

The launcher is the single point of failure. Upon failure the application needs to be restarted by the user.

## 4.7 Dynamic load balancing

As already mentioned, runners send to the server the dynamic state of each member. For the sole purpose of DA, only the sub-part of this dynamic state that we call the assimilated state would actually be necessary. But having the full dynamic state on the server side brings an additional level of flexibility central to the Melissa-DA architecture: runners become agnostic of the members they propagate. We rely on this property for the dynamic load balancing mechanism of Melissa-DA.

Dynamic load balancing is a very desirable feature when the propagation time of the different members differ. This is typically the case with solvers relying on iterative methods, but also when runners are started on heterogeneous resources, for instance nodes with GPUs versus nodes without, or if the network topology impacts unevenly the data transfer time between the server and runners. The server has to wait for the last member to return its background state before being able to proceed with the update phase computing the analysis states. The worst case occurs when state propagation is fully parallel, i.e. when each runner is in charge of a single member. In that case runner idle time is the sum of the differences between each propagation time and the slowest one. As we target large numbers of members, each member potentially being a large-scale parallel simulation, this can account for significant resource under utilization (Figure 7 gives a view of this effect for a simulated execution trace for ParFlow). To reduce this source of inefficiency Melissa-DA enables 1) to control the propagation concurrency level independently from the number of members 2) to distribute dynamically members to runners.

The Melissa-DA load balancing strategy relies on the GRAHAM list scheduling algorithm [14]. The server distributes the members to runners on a first come first serve basis. Each time a runner becomes idle, the server provides it with the dynamic state of one member to propagate. This algorithm is simple to implement, has a very low operational cost, and does not require any information on the member propagation time. The performance of the list scheduling algorithm is guaranteed to be at worst twice the one of the optimal scheduling that requires to know the member execution time. More precisely the wall-time  $T_{ls}$  (called makespan in the scheduling jargon) is bounded by the optimal

walltime  $T_{opt}$ :

$$T_{ls} \leq T_{opt} * (2 - \frac{1}{m}) \quad (3)$$

where  $m$  is the number of machines used, in our case the number of runners [36]. This bound is tight, i.e. cannot be lowered, as there exist instances where this bound is actually met.

A static scheduling distributing evenly the members to runners at the beginning of each propagation phase, does not guarantee the same efficiency as long as we have no knowledge on the member propagation time. The worst case occurs if one runner gets the members with the longest propagation time.

Also the list scheduling algorithm is efficient independent of the number of runners, combining well with the Melissa-DA runner management strategy. The number of expected runners is statically defined by the user at start time. But the actual number of executed runners depends on the machine availability and batch scheduler. Runners can start at different time periods, they may not all run due to resource limitations, some may crash and try to restart. With list scheduling, a runner gets from the server the next member to propagate as soon as connected and ready.

From this base algorithm several optimizations can be considered. In particular data movements could be reduced by trying to avoid centralizing all dynamic states on the runner using decentralized extensions of list scheduling like work stealing [9]. This could be beneficial when the assimilated state only represents a small fraction of the dynamic state. This is left as a future work.

## 4.8 Code

The code of Melissa-DA (server and API) is written in C++, relying on features introduced with cpp14. This is especially handy regarding smart pointers to avoid memory leaks and having access to different containers (sets, lists, maps) used to store scheduling mappings. The assimilation update phase is contained in its own class deriving the `Assimilator`-interface, which accesses the received dynamic states and creates a new set of analysis states to be propagated.

Implementing new ensemble-based DA methods within the Melissa-DA framework is straightforward, requiring to specify how to initialize the ensemble and how to transform the ensemble of background states in an ensemble of analysis states using observations.

A derived class calling the PDAF EnKF update phase methods was implemented and is linked against the user defined methods to initialize the ensemble and observations and to apply the observation operator (Figure 3). From PDAF perspective, the Melissa-DA server acts as a parallel simulation code assembling a "flexible assimilation system" with one model instance propagating all ensemble members sequentially online<sup>2</sup>. By handling the server MPI communicator to PDAF, the update phase is parallelized on all server cores.

<sup>2</sup>see <http://pdaf.awi.de/trac/wiki/ModifyModelforEnsembleIntegration>, retrieved the 25.08.2020



To let Melissa-DA support other assimilation algorithms implemented in PDAF (e.g., LEnKF, LETKF...<sup>3</sup>) only classes inheriting the `Assimilator` interface with calls to the desired PDAF filter update methods must be implemented.

The Melissa-DA launcher is written in Python. To execute a Melissa-DA study, a user typically executes a Python script for configuring the runs, importing the launcher module and launching the study.

The Melissa-DA code base contains a test suite allowing end-to-end testing against results retrieved using PDAF as reference implementation. The test suite also contains test cases validating recovery from induced runner and server faults.

The Melissa-DA code base will be made open source on GitHub upon publication.

## 5 Experimental study

Experiments in [subsection 5.5](#) and [subsection 5.6](#) were performed on the Jean-Zay supercomputer on up to 424 of the 1,528 scalar compute nodes. Each node has 192 GB of memory and two Intel Cascade Lake processors with 40 cores at 2.5 GHz. The compute nodes are connected through an Omni-Path interconnection network with a bandwidth of 100 Gb/s. The other experiments ran on the JUWELS supercomputer (2 Intel Xeon processors, in total 48 cores at 2.7 GHz and 96 GB of memory per compute node, EDR-Infiniband (Connect-X4)) [\[18\]](#).

For all experiments we keep nearly the same problem size. Experiments assimilating ParFlow simulations use an assimilated state vector of 4,031,700 cells (pressure, 4,031,700 doubles,  $\approx 30.8$  MiB), representing the Neckar catchment in Germany. For our test we were provided observations from 25 ground water measuring sensors distributed over the whole catchment. Observation values were taken from a virtual reality simulation [\[35\]](#). The dynamic state contains the pressure, saturation and density vectors for a total size of  $\approx 92.4$  MiB). ParFlow runners are parallelized on one full node (40 processes for experiments on Jean-Zay and 48 processes for JUWELS respectively). For the experiments profiling the EnKF update phase ([subsection 5.3](#)), a toy model from the PDAF examples, parallelized only on half of a node's cores, is used to save compute hours. For this experiment the dynamic state equals the assimilated state (4,032,000 grid cells,  $\approx 30.8$  MiB). The `init_ensemble` function uses an online approach relying on one initial system state adding some uniform random noise for each member. Loading terabytes of data for the initial ensemble states is thus avoided. To further avoid the influence from file system jitter, assimilation output to disk is deactivated in the following performance measurements.

<sup>3</sup>for a complete list see <http://pdaf.awi.de/trac/wiki/FeaturesofPdaf>, retrieved the 25.08.2020

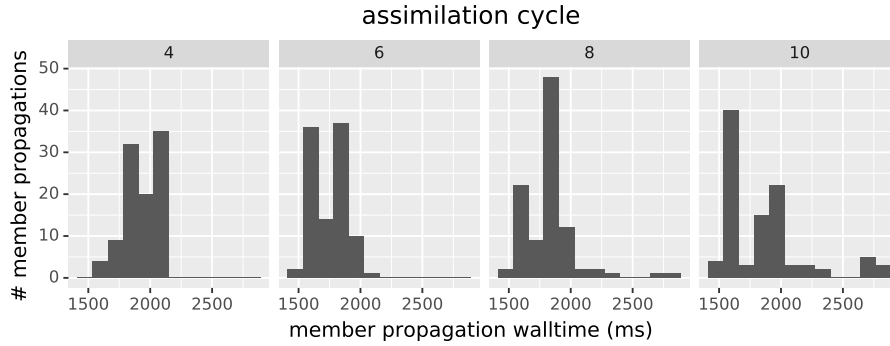


Figure 4: Histogram of propagation walltimes for 100 members during multiple assimilation cycles

For the sake of simplicity and minimal intrusion, the code was instrumented by calls to the STL-chrono library<sup>4</sup>, allowing a precision of a nanosecond for these measurements. This minimal instrumentation was successfully validated against measurements using automatic Score-P instrumentation and Scalasca [20].

### 5.1 ParFlow

For first tests we assimilate ParFlow simulations with Melissa-DA. ParFlow is a physically based, fully coupled water transfer model for the critical zone that relies on an iterative Krylov-Newton solver [3, 17, 27, 21, 26]. This solver performs a changing amount of iterations until a defined convergence tolerance is reached at each timestep.

### 5.2 Ensemble propagation

Figure 4 shows the walltime distribution of 100 ParFlow member propagations for multiple assimilation cycles. The propagation time can vary significantly from about 1.5s to 2.5s, with an average at 1.9s. The main cause for these fluctuations is the Krylov-Newton solver used by ParFlow that converges with different number of iterations depending on the member state. As detailed in subsection 4.7, these variations can impair the execution efficiency. Melissa-DA mitigates this effect by dynamically distributing members to runners following a list scheduling algorithm.

### 5.3 EnKF ensemble update

Figure 5 displays the evolution of the update phase walltime depending on the number of members, using Melissa-DA with the PDAF implementation of EnKF. The mean is computed over 25 assimilation cycles, assimilating 288 observations each time. Standard deviation is omitted as not being significant (< 6% of the update phase walltime). The EnKF update phase is executed

<sup>4</sup>see <https://en.cppreference.com/w/cpp/chrono>, retrieved the 24.06.2020

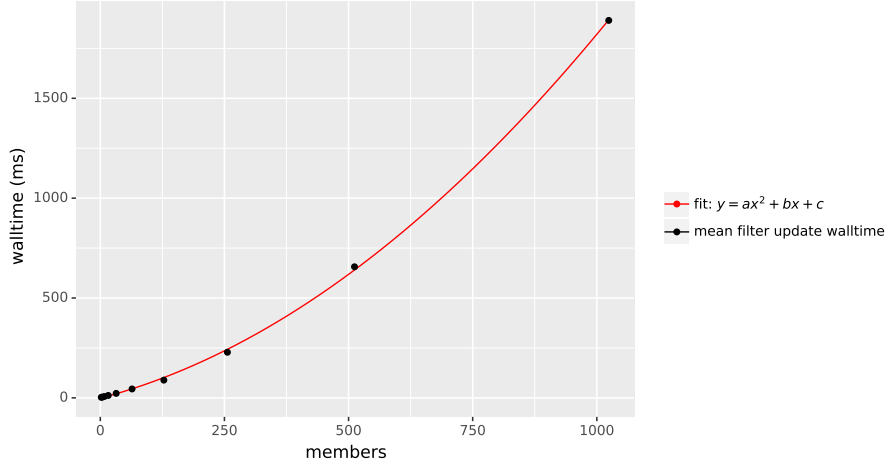


Figure 5: Assimilating 288 observations into about 4M grid cells with up to 1,024 members on JUWELS. Mean over 25 update phase walltimes.

on 3 JUWELS nodes (144 cores in total). The EnKF update phase relies on the calculation of covariance matrices over  $M$  samples resulting in a computational complexity for the EnKF update phase of  $O(M^2)$ ,  $M$  being the amount of ensemble members. This is confirmed by the experiments that fit a square function. The walltime of the update phase also depends on the amount of observations. In the following experiments less observations are used, leading to an update phase of about only 1.1 seconds.

We also performed a strong scaling study (Figure 6) timing the update phase for 1,024 members and a varying number of server cores. The parallelization leads to walltime gains up to 576 cores. Computing the covariance matrix for update phase is known to be difficult to efficiently parallelize. Techniques like localization enable to push the scalability limit. Localization is not used in this paper as we run with a limited number of observations. As Melissa-DA relies on PDAF which supports localization, localization can be easily activated by changing the API calls to PDAF in the Melissa-DA **Assimilator** interface. Refer to [31] and [30] for further EnKF/PDAF scaling experiments.

Dimensioning the Melissa-DA server optimally depends on the assimilated problem dimensions, the used assimilation algorithm and the target machine. It should be examined in a quick field study before moving to production. The results of such a field study can be seen in Figure 6, *bottom*. In the depicted case less core hours are consumed when not using a large number of server nodes (and cores respectively) since these are idle during the whole propagation phase outplaying the walltime advantage they bring during the update phase. For the following experiments we assume that the update phase is short compared to the propagation phase leading to the policy: Use the least server nodes possible to fulfill memory requirements. If the server would be faster using a sub-part of the cores available per node, use less cores (e.g., only 24 or 12 cores per server

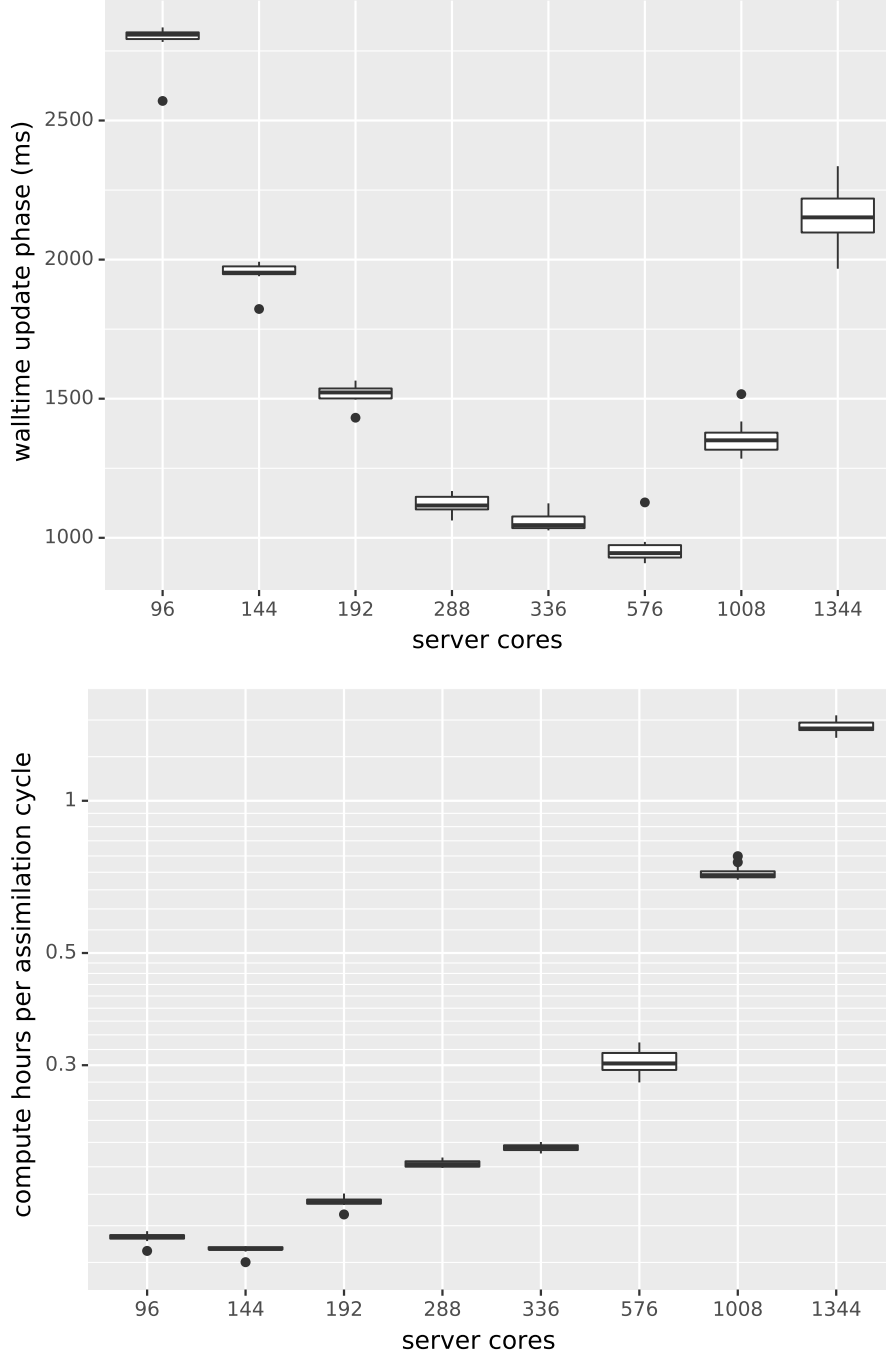


Figure 6: Boxplot of the update phase walltime (*top*) and the total compute hours per assimilation cycle (comprising update and propagation phase, *bottom*) when assimilating 288 observations into about 4 M grid cells with 1,024 members with a varying number of server cores on JUWELS. The latter graph can be used to evaluate server dimensioning.

node). Some supercomputers provide special large memory nodes that could be leveraged to run the Melissa-DA server.

## 5.4 Runner scaling

We now focus on the member to runner ratio. A single runner avoids idle runner time during the propagation phase, while having as many runners as members ensures the shortest propagation time but maximizes idle time (Figure 7). Idle time also come from the switch between propagation and update phases: the server is mostly inactive during the propagation phase, while, in opposite runners are inactive during the update phase.

We experiment with a varying number of runners for a fixed number of members (100 and 1,024) and a given server configuration (Figure 8). Plotted values result from an average obtained from 8 executions, taking for each execution the time of the 2 last, over 3, assimilation cycles. The efficiency of the update phase (Figure 8 top) is computed against the time obtained by running the members on a single runner. The compute hours are the total amount of consumed CPU resources (update and propagation phase, runners and server) during the assimilation cycles. For both plots, standard deviations are omitted as being small (relative standard deviations ( $\frac{\text{standard deviation}}{\text{mean}}$ ) always smaller than 3%). The server was scaled to meet the memory needs. For the 100 (resp. 1024) member case, the server ran with 48 (resp. 240) cores on one (resp. 5) nodes. Each runner is executed on 48 cores (1 node).

Efficiency stays beyond 90%, when each runner propagates at least 7 or 8 members, 95% for more than 10 members per runner and close to 100% for 50 or 100 members per runner. This demonstrates the efficiency of Melissa-DA load balancing algorithm that maintains high efficiencies down to a relatively small number of members per runner. Obviously these levels of efficiency also depend on the distribution of propagation walltimes (see subsection 5.2).

But the resources used for the server also need to be considered. The total amount of compute hours (Figure 8 bottom) shows a U shape curve with a large flatten bottom at about 9 members per runner for the 100 members case and at about 20 for the 1,024 members case: a sufficiently large number of runners is required to amortize the server cost. Changing the runner amount around those sweet spots changes significantly the efficiency of the update phase but slightly impacts the total compute hours: the efficiency variation is compensated by the impact on the server idle time during the update phase that varies inversely (the server is mostly idle during this phase). This also shows that changing the number of runners in these areas is efficient. This advocates for leveraging Melissa-DA elasticity for adding/removing runners according to machine availability.

If we look at the compute hours, the  $10\times$  increase in the number of members to propagate roughly matches the increase in compute hours. Thus the resource usage is here dominated by the propagation phase and the server does not appear as a bottleneck.

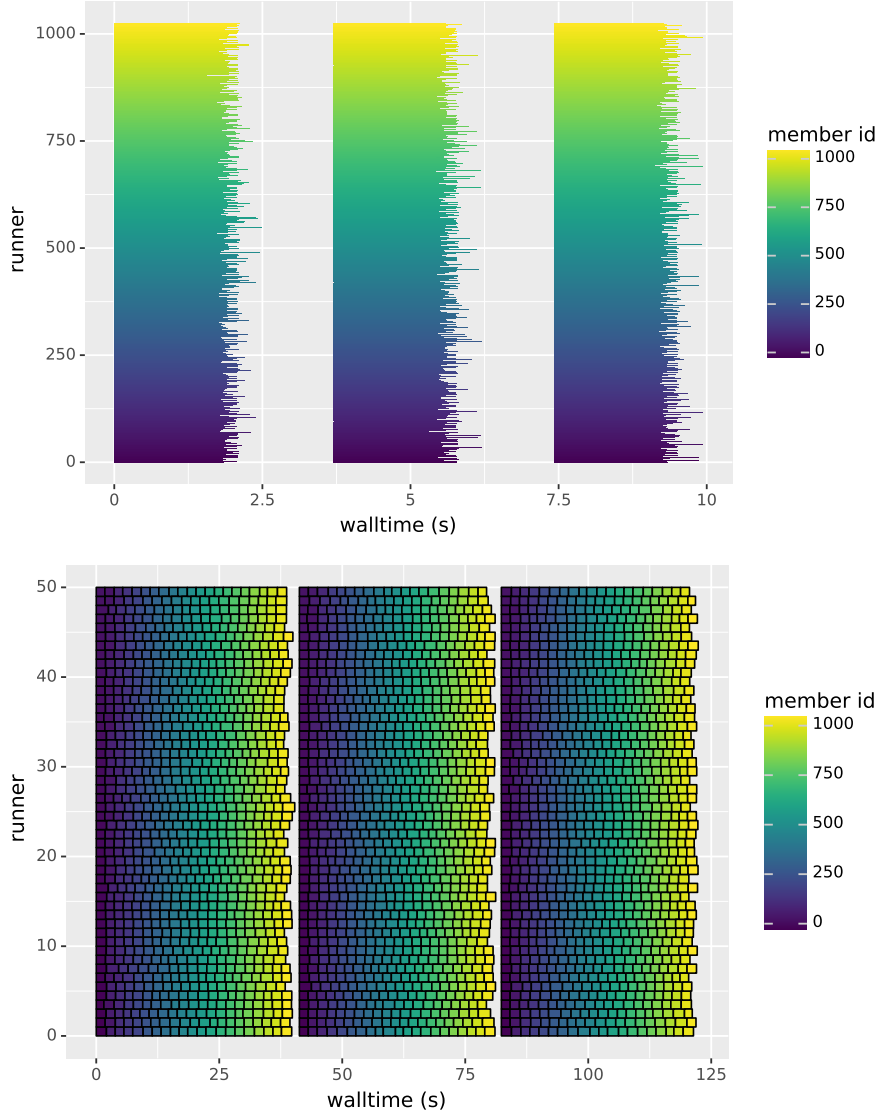


Figure 7: Load balancing 1,024 members with list scheduling on 50 (bottom) and 1,024 runners (top). Three assimilation cycles are plotted. Simulated execution, based on member propagation walltimes from [Figure 4](#). Runners are idle about 50% of the time when each one propagates a single member (top), while idle time is reduced to 6% when each runner propagates about 20 members (bottom).

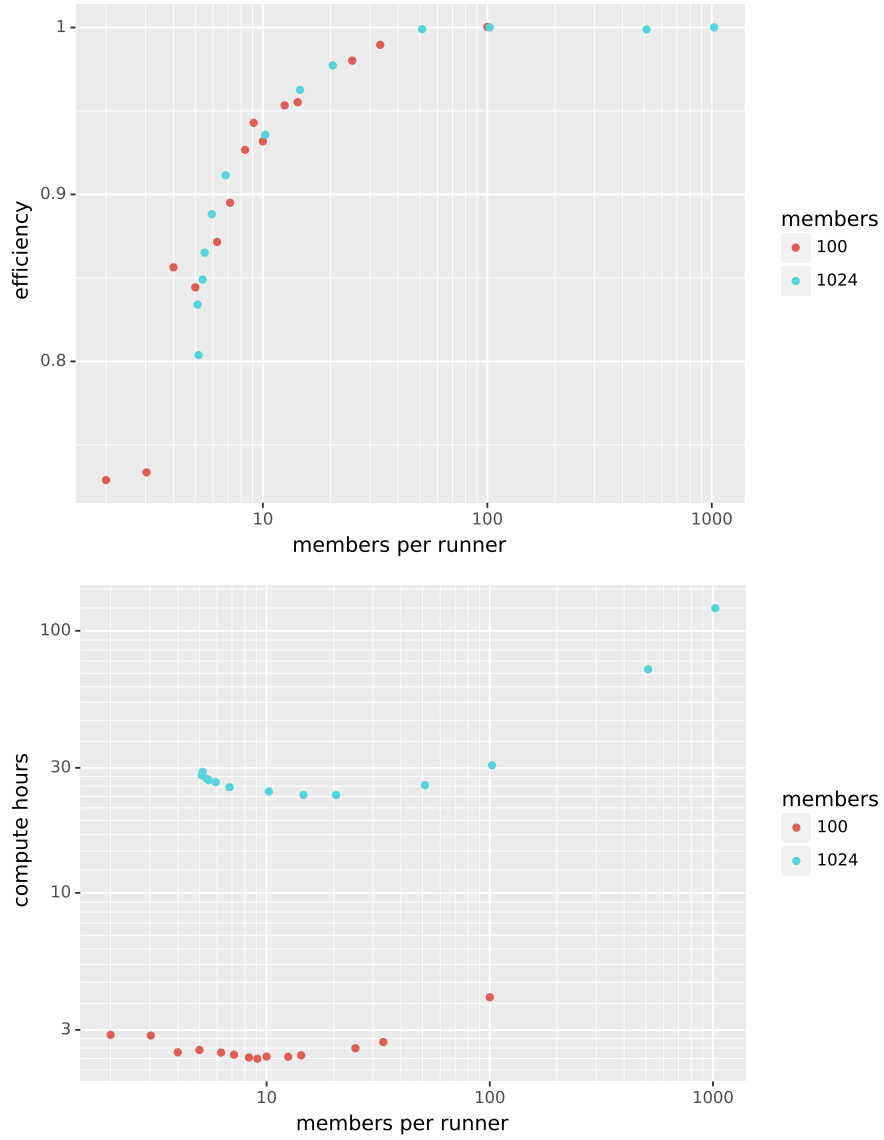


Figure 8: Efficiency of the propagation phase only (*top*) and total compute hours used per assimilation cycle (update and propagation phase) (*bottom*) for different numbers of runners while assimilating 25 observations into an about 4 M grid cell ParFlow simulation with 100 and 1,024 ensemble members.

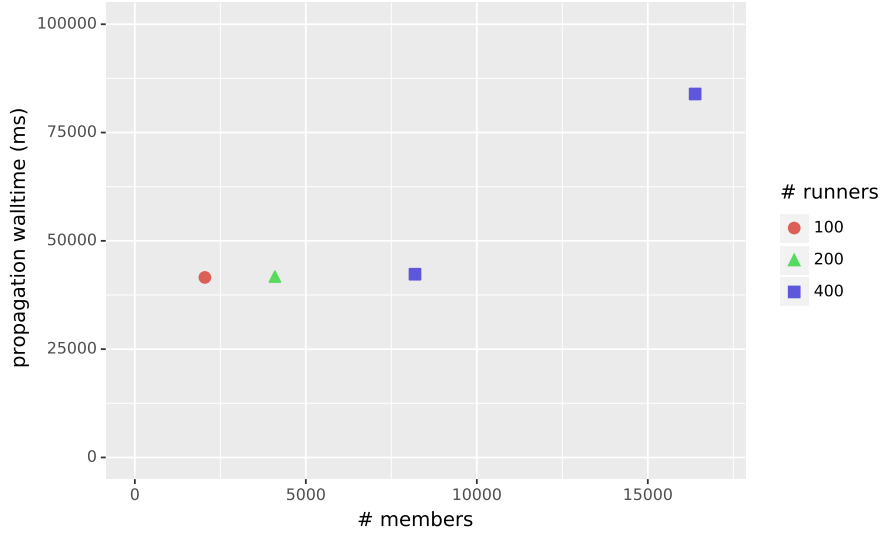


Figure 9: Scaling the assimilation of the ParFlow domain on up to 16,384 members

The server exchanges about 92 MiB of state data per member and assimilation cycle. Up to 24 (resp. 96) states are assimilated per second for the 100 (resp. 1,024) members case (propagation *and* update phase) using about 2 (resp. 5) members per runner.

## 5.5 Ultra-large ensembles

In this section we scale Melissa-DA to ultra-large ensembles, assimilating with up to 16,384 members. To save compute hours only a few assimilation cycles ran on up to 424 compute nodes using up to 16,240 cores of the Jean Zay supercomputer. When doubling both, the ensemble size and the number of runners, the execution time stays roughly the same, with an average number of about 20 members per runner. The number of runners was not increased when running 16,384 members, as we were not able to get the necessary resource allocation on the machine. Thus, the walltime doubles. Notice that we plot only the second assimilation cycle as the first cycle shows higher execution times as not all runners are connected to the server yet.

For each assimilation cycle with 16,384 members, a total of 2.9 TiB of dynamic state data (0.96 TiB being assimilated data) are transferred back and forth over the network between the server and all the runners. By enabling direct data transfers, Melissa-DA avoids the performance penalty that would induce the use of files as intermediate storage.

The server is spread on the minimum number of nodes necessary to fulfill the memory requirements (1.9 TiB to hold the dynamic states of the 16,384 ensemble members). Since Melissa-DA and the underlying PDAF assimilation engine parallelization are based on domain decomposition and the domain size



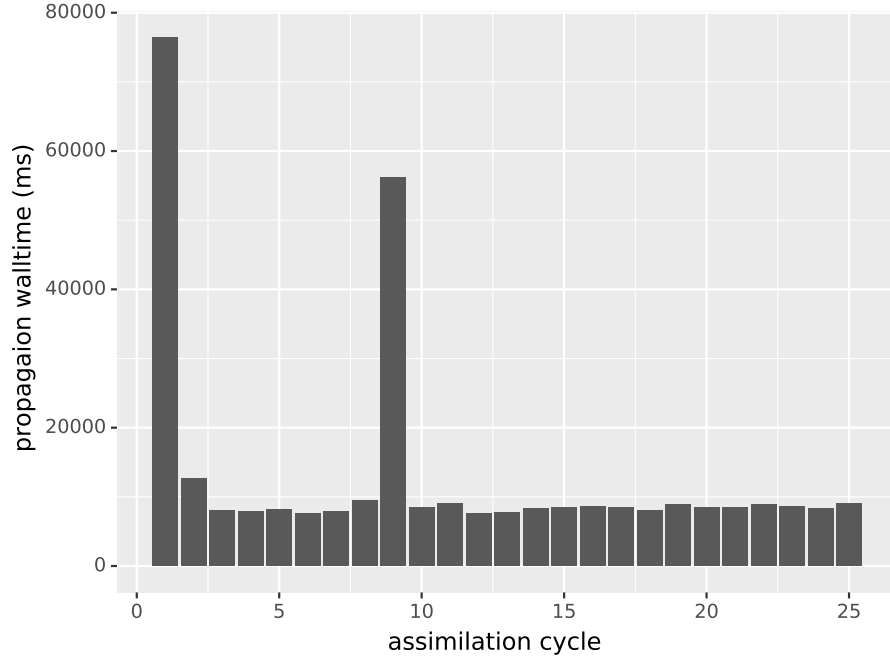


Figure 10: Walltime of the propagation phase over different cycles for one ParFlow assimilation (30 ensemble members, 9 runners at the beginning, 1 server node). Higher propagation walltimes are due to a lower number of active runners not all ready from the beginning (first and second cycles) or after a crash (9<sup>th</sup> cycle).

does not change when the number of members goes up, the number of allocated server processes is kept constant at 240 cores. Thus the update phase takes a considerable amount of the application walltime (up to 53s for the 16,384 members case). Future work will look at using techniques like localization to reduce the cost of the update phase. As being supported by PDAF, this should not entail any modification to Melissa-DA.

## 5.6 Fault tolerance and elasticity

Runners can be dynamically added or removed, giving the Melissa-DA elasticity. Also the fault tolerance protocol benefits of this feature. This simple experiment on one execution aims to demonstrate the Melissa-DA elasticity (Figure 10). The first and second propagation phase take longer since not all runners are ready to accept members from the beginning (respectively about 80s and 13s) instead of less than 10s. At the 9<sup>th</sup> assimilation cycle, 4 out of 9 runners are killed. The timeout for runner fault detection was set to 25s. When the server detects the runner faults, their member propagations are rescheduled to other runners. At the same time the launcher also detects these faults and restarts 4

runners. Restarting took place within 55 s after the runner crashes. Already at the 10<sup>th</sup> propagation phase 9 runners are propagating members again.

Notice that here we leverage the batch scheduler capabilities (Slurm). A single allocation encompassing all necessary resources is requested at the beginning. Next jobs for the server or runners are allocated by Slurm within this envelope, ensuring a fast allocation. When the runners crash, again the restarted runners reuse the same envelope. A hybrid scheme is also possible, requesting a minimal first allocation to ensure the data assimilation to progress fast enough, while additional runners are allocated outside the envelope but whose availability to accept members may take longer depending on the machine load. It is planned to rely in such situations on *best effort* jobs that are supported by batch schedulers like OAR [10]. Best effort jobs can be deleted by the batch scheduler whenever resources to start other higher prioritized jobs are needed. This way Melissa-DA runners can fill up underutilized resources between larger job allocations on the cluster. All these variations on the allocation scheme require only minimal customization of the assimilation study configuration.

## 6 Conclusion

In this article we introduced Melissa-DA, an elastic, fault-tolerant, load balancing, online framework for ensemble-based DA. All these properties lead to an architecture allowing to run Ensemble Kalman Filters with up to 16,384 members to assimilate observations into large-scale simulation state vectors of more than 4 M degrees of freedom. At the same time Melissa-DA scaled up to 16,240 compute cores.

Thanks to the master/worker architecture adding and removing resources to the Melissa-DA application is possible at runtime. In future we want to profit from this agile adaptation to further self-optimize the compute hour consumption. We will also consider executions on heterogeneous machines (nodes with accelerators or more memory). The modular master/worker model of Melissa-DA allows for flexibility to leverage such architectures. Large memory nodes for the server can also have a very positive impact on the core hour consumption. We are also planning to integrate other assimilation methods into Melissa-DA and to run use cases with diverse more complex simulation codes and at different scales.

Concerned with measuring the compute cost and environmental impact of this paper, we counted the total number of CPU hours used, including all intermediate and failed tests that do not directly appear in this paper, at about 136,000 CPU hours split between the JUWELS and the Jean-Zay supercomputers.

## Acknowledgements

We would like to thank the following people: Bibi Naz, Ching Pui Hung and Harrie-Jan Hendricks Franssen from Fohrschungszentrum Juelich for the scientific exchange as well as for providing the ParFlow real world use case for data assimilation, Kai Keller and Leonardo Bautista-Gomez from Barcelona Supercomputing Center for the integration of FTI into the Melissa-DA server code as well as Lars Nerger from Alfred Wegener Institut and Wolfgang Kurtz from Leibniz Supercomputing Center for the scientific exchange on PDAF, ParFlow and TerrSysMP. We also thank the DataMove research engineers Christoph Conrads and Théophile Terraz for contributing to the Melissa-DA software stack and proof reading.

## Funding

This project has received funding from the European Union’s Horizon 2020 research and innovation program under grant agreement No 824158 (EoCoE-2). This work was granted access to the HPC resources of IDRIS under the allocation 2020-A8 A0080610366 attributed by GENCI (Grand Equipement National de Calcul Intensif).

## References

- [1] Jeffrey Anderson, Tim Hoar, Kevin Raeder, Hui Liu, Nancy Collins, Ryan Torn, and Avelino Avellano. The Data Assimilation Research Testbed: A Community Facility. *Bulletin of the American Meteorological Society*, 90(9):1283–1296, September 2009. Publisher: American Meteorological Society.
- [2] Mark Asch, Marc Bocquet, and Maëlle Nodet. *Data assimilation: methods, algorithms, and applications*, volume 11. SIAM, 2016.
- [3] Steven F. Ashby and Robert D. Falgout. A Parallel Multigrid Preconditioned Conjugate Gradient Algorithm for Groundwater Flow Simulations. *Nuclear Science and Engineering*, 124(1):145–159, September 1996.
- [4] Yadu Babuji, Anna Woodard, Zhuozhao Li, Daniel S. Katz, Ben Clifford, Rohan Kumar, Luksaz Lacinski, Ryan Chard, Justin M. Wozniak, Ian Foster, Michael Wilde, and Kyle Chard. Parsl: Pervasive parallel programming in python. In *28th ACM International Symposium on High-Performance Parallel and Distributed Computing (HPDC)*, 2019.
- [5] Vivek Balasubramanian, Travis Jensen, Matteo Turilli, Peter Kasson, Michael Shirts, and Shantenu Jha. Adaptive ensemble biomolecular applications at scale. *SN Computer Science*, 1(2):1–15, 2020.

- [6] Vivek Balasubramanian, Matteo Turilli, Weiming Hu, Matthieu Lefebvre, Wenjie Lei, Guido Cervone, Jeroen Tromp, and Shantenu Jha. Harnessing the power of many: Extensible toolkit for scalable ensemble applications. In *IPDPS 2018*, 2018.
- [7] Leonardo Bautista-Gomez, Seiji Tsuboi, Dimitri Komatitsch, Franck Cappello, Naoya Maruyama, and Satoshi Matsuoka. FTI: High performance Fault Tolerance Interface for hybrid systems. In *SC '11: Proceedings of 2011 International Conference for High Performance Computing, Networking, Storage and Analysis*, pages 1–12, November 2011.
- [8] Jonas Berndt. *On the predictability of exceptional error events in wind power forecasting —an ultra large ensemble approach—*. PhD thesis, Universität zu Köln, 2018.
- [9] Robert D. Blumofe and Charles E. Leiserson. Scheduling multithreaded computations by work stealing. *J. ACM*, 46(5):720–748, 1999.
- [10] Nicolas Capit, Georges Da Costa, Yiannis Georgiou, Guillaume Huard, Cyrille Martin, Grégory Mounié, Pierre Neyron, and Olivier Richard. A batch scheduler with high level components. In *Cluster computing and Grid 2005 (CCGrid05)*, Cardiff, United Kingdom, 2005. IEEE.
- [11] A. M. Clayton, A. C. Lorenc, and D. M. Barker. Operational implementation of a hybrid ensemble/4D-Var global data assimilation system at the Met Office. *Quarterly Journal of the Royal Meteorological Society*, 139(675):1445–1461, July 2013.
- [12] Wael R Elwasif, David E Bernholdt, Sreekanth Pannala, Srikanth Allu, and Samantha S Foley. Parameter sweep and optimization of loosely coupled simulations using the dakota toolkit. In *Computational Science and Engineering (CSE), 2012 IEEE 15th International Conference on*, pages 102–110, 2012.
- [13] Geir Evensen. *Data assimilation: the ensemble Kalman filter*. Springer Science & Business Media, 2009.
- [14] R. L. Graham. Bounds for Certain Multiprocessing Anomalies. *Bell System Technical Journal*, 45(9):1563–1581, 1966.
- [15] Pieter Hintjens. *ZeroMQ, Messaging for Many Applications*. O’Reilly Media, 2013.
- [16] Pieter Leopold Houtekamer, Mark Buehner, and Michèle De La Chevrotière. Using the hybrid gain algorithm to sample data assimilation uncertainty. *Quarterly Journal of the Royal Meteorological Society*, 145(S1):35–56, 2019.

- [17] Jim E. Jones and Carol S. Woodward. Newton–Krylov-multigrid solvers for large-scale, highly heterogeneous, variably saturated flow problems. *Advances in Water Resources*, 24(7):763–774, July 2001.
- [18] Jülich Supercomputing Centre. JUWELS: Modular Tier-0/1 Supercomputer at the Jülich Supercomputing Centre. *Journal of large-scale research facilities*, 5(A135), 2019.
- [19] Rudolph Emil Kalman. A new approach to linear filtering and prediction problems. *Transactions of the ASME–Journal of Basic Engineering*, 82(Series D):35–45, 1960.
- [20] Andreas Knüpfer, Christian Rössel, Dieter an Mey, Scott Biersdorff, Kai Diethelm, Dominic Eschweiler, Markus Geimer, Michael Gerndt, Daniel Lorenz, Allen Malony, Wolfgang E. Nagel, Yury Oleynik, Peter Philippen, Pavel Saviankou, Dirk Schmidl, Sameer Shende, Ronny Tschüter, Michael Wagner, Bert Wesarg, and Felix Wolf. Score-P: A Joint Performance Measurement Run-Time Infrastructure for Periscope, Scalasca, TAU, and Vampir. In Holger Brunst, Matthias S. Müller, Wolfgang E. Nagel, and Michael M. Resch, editors, *Tools for High Performance Computing 2011*, pages 79–91, Berlin, Heidelberg, 2012. Springer.
- [21] Stefan J. Kollet and Reed M. Maxwell. Capturing the influence of groundwater dynamics on land surface processes using an integrated, distributed watershed model. *Water Resources Research*, 44(2):W02402, February 2008.
- [22] Els Kooij-Connally. Technical Memorandum. page 44, 2017.
- [23] W. Kurtz, G. He, S. J. Kollet, R. M. Maxwell, H. Vereecken, and H.-J. Hendricks Franssen. TerrSysMP-PDAF (version 1.0): a modular high-performance data assimilation framework for an integrated land surface–subsurface model. *Geosci. Model Dev.*, 9(4):1341–1360, April 2016.
- [24] Eric Liang, Richard Liaw, Robert Nishihara, Philipp Moritz, Roy Fox, Ken Goldberg, Joseph Gonzalez, Michael Jordan, and Ion Stoica. Rllib: Abstractions for distributed reinforcement learning. In *International Conference on Machine Learning*, pages 3053–3062, 2018.
- [25] Edward N. Lorenz. Deterministic Nonperiodic Flow. *Journal of the Atmospheric Sciences*, 20(2):130–141, March 1963. Publisher: American Meteorological Society.
- [26] Reed M. Maxwell. A terrain-following grid transform and preconditioner for parallel, large-scale, integrated hydrologic modeling. *Advances in Water Resources*, 53:109–117, March 2013.
- [27] Reed M. Maxwell and Norman L. Miller. Development of a Coupled Land Surface and Groundwater Model. *Journal of Hydrometeorology*, 6(3):233–247, June 2005.

- [28] Takemasa Miyoshi, Keiichi Kondo, and Toshiyuki Imamura. The 10,240-member ensemble Kalman filtering with an intermediate AGCM: 10240-MEMBER ENKF WITH AN AGCM. *Geophysical Research Letters*, 41(14):5264–5271, July 2014.
- [29] Philipp Moritz, Robert Nishihara, Stephanie Wang, Alexey Tumanov, Richard Liaw, Eric Liang, Melih Elibol, Zongheng Yang, William Paul, Michael I. Jordan, and Ion Stoica. Ray: a distributed framework for emerging AI applications. In *Proceedings of the 13th USENIX conference on Operating Systems Design and Implementation*, OSDI’18, pages 561–577, Carlsbad, CA, USA, October 2018. USENIX Association.
- [30] L. Nerger, W. Hiller, and J. Schröter. PDAF - THE PARALLEL DATA ASSIMILATION FRAMEWORK: EXPERIENCES WITH KALMAN FILTERING. In *Use of High Performance Computing in Meteorology*, pages 63–83, Reading, UK, September 2005. WORLD SCIENTIFIC.
- [31] Lars Nerger and Wolfgang Hiller. Software for ensemble-based data assimilation systems—implementation strategies and scalability. *Computers & Geosciences*, 55:110–118, 2013.
- [32] Ioannis Paraskevagos, Andre Luckow, Mahzad Khoshlessan, George Chantzialexiou, Thomas E Cheatham, Oliver Beckstein, Geoffrey C Fox, and Shantenu Jha. Task-parallel analysis of molecular dynamics trajectories. In *Proceedings of the 47th International Conference on Parallel Processing*, pages 1–10, 2018.
- [33] S. Pronk, G. R. Bowman, B. Hess, P. Larsson, I. S. Haque, V. S. Pande, I. Pouya, K. Beauchamp, P. M. Kasson, and E. Lindahl. Copernicus: A new paradigm for parallel adaptive molecular dynamics. In *2011 International Conference for High Performance Computing, Networking, Storage and Analysis (SC)*, pages 1–10, Nov 2011.
- [34] Matthew Rocklin. Dask: Parallel computation with blocked algorithms and task scheduling. In Kathryn Huff and James Bergstra, editors, *Proceedings of the 14th Python in Science Conference*, pages 130 – 136, 2015.
- [35] Bernd Schalge, Gabriele Baroni, Barbara Haese, Daniel Erdal, Gernot Geppert, Pablo Saavedra, Vincent Haefliger, Harry Vereecken, Sabine Attinger, Harald Kunstmann, Olaf A. Cirpka, Felix Ament, Stefan Kollet, Insa Neuweiler, Harrie-Jan Hendricks Franssen, and Clemens Simmer. Presentation and discussion of the high resolution atmosphere-land surface subsurface simulation dataset of the virtual Neckar catchment for the period 2007-2015. *Earth System Science Data Discussions*, pages 1–40, March 2020. Publisher: Copernicus GmbH.
- [36] D.B. Shmoys, J. Wein, and D.P. Williamson. Scheduling parallel machines on-line. In *[1991] Proceedings 32nd Annual Symposium of Foundations*

- of Computer Science*, pages 131–140, San Juan, Puerto Rico, 1991. IEEE Comput. Soc. Press.
- [37] Théophile Terraz, Alejandro Ribes, Yvan Fournier, Bertrand Iooss, and Bruno Raffin. Melissa: Large scale in transit sensitivity analysis avoiding intermediate files. In *International Conference for High Performance Computing, Networking, Storage and Analysis (SC'17)*, Denver, 2017.
  - [38] Habib Toye, Samuel Kortas, Peng Zhan, and Ibrahim Hoteit. A fault-tolerant hpc scheduler extension for large and operational ensemble data assimilation: Application to the red sea. *Journal of Computational Science*, 27:46 – 56, 2018.
  - [39] Nils van Velzen, Muhammad Umer Altaf, and Martin Verlaan. OpenDA-NEMO framework for ocean data assimilation. *Ocean Dynamics*, 66(5):691–702, May 2016.
  - [40] Lin Zhang, Yongzhu Liu, Yan Liu, Jiandong Gong, Huijuan Lu, Zhiyan Jin, Weihong Tian, Guiqing Liu, Bin Zhou, and Bin Zhao. The operational global four-dimensional variational data assimilation system at the China Meteorological Administration. *Quarterly Journal of the Royal Meteorological Society*, 145(722):1882–1896, 2019.



**RESEARCH CENTRE  
GRENOBLE – RHÔNE-ALPES**

Inovallée  
655 avenue de l'Europe Montbonnot  
38334 Saint Ismier Cedex

Publisher  
Inria  
Domaine de Voluceau - Rocquencourt  
BP 105 - 78153 Le Chesnay Cedex  
[inria.fr](http://inria.fr)

ISSN 0249-6399